HHS Public Access

Author manuscript

Oncogene. Author manuscript; available in PMC 2019 December 24.

Published in final edited form as:

Oncogene. 2019 July ; 38(29): 5805–5816. doi:10.1038/s41388-019-0843-1.

Activation of IGF1R by DARPP-32 promotes STAT3 signaling in gastric cancer cells

Shoumin Zhu[1], **Mohammed Soutto**[1,2], **Zheng Chen**[1,2], **M. Blanca Piazuelo**[4], **M. Kay Washington**[5], **Abbes Belkhiri**[6], **Alexander Zaika**[1,2,3], **Dunfa Peng**[1,3], and **Wael El-Rifai**[1,2,3,*]

[1]Department of Surgery, Miller School of Medicine, University of Miami, Miami, Florida, USA.

[2]Department of Veterans Affairs, Miami Healthcare System, Miami, Florida, USA.

[3]Sylvester Comprehensive Cancer Center, University of Miami, Miami, Florida, USA.

[4]Department of Medicine, Vanderbilt University Medical Center, Nashville, Tennessee, USA

[5]Department of Pathology, and Vanderbilt University Medical Center, Nashville, Tennessee, USA

[6]Department of Surgery, Vanderbilt University Medical Center, Nashville, Tennessee, USA

Abstract

Dopamine and cAMP-regulated phosphoprotein, Mr 32000 (DARPP-32), is frequently overexpressed in earlt stages of gastric cancers. We utilized *in vitro* assays, 3D gastric gland organoid cultures, mouse models, and human tissue samples to investigate the biological and molecular impact of DARPP-32 on activation of IGF1R and STAT3 signaling and gastric tumorigenesis. DARPP-32 enhanced phosphorylation of IGF1R (Y1135), a step that was critical for STAT3 phosphorylation at Y705, nuclear localization, and transcription activation. By using proximity ligation and co-immunoprecipitation assays, we found that IGF1R and DARPP-32 co-existed in the same protein complex. Binding of DARPP-32 to IGF1R promoted IGF1R phosphorylation with subsequent activation of downstream SRC and STAT3. Analysis of gastric tissues from the TFF1 knockout (KO) mouse model of gastric neoplasia, demonstrated phosphorylation of STAT3 in the early stages of gastric tumorigenesis. By crossing the TFF1 KO mice with DARPP-32 (DP) knockout (KO) mice, that have normal stomach, we obtained double knockout (TFF1 KO/DP KO). The gastric mucosa from the double KO mice did not show phosphorylation of IGF1R or STAT3. In addition, the TFF1 KO/DP KO mice had significant delay in developing neoplastic gastric lesions. Analysis of human gastric cancer tissue microarrays, showed high levels of DARPP-32 and positive immunostaining for nuclear STAT3 in cancer tissues, as compared to non-cancer histologically normal tissues. In summary, the presence of a signaling axis mediated by DARPP-32–IGF1R is a critical step in gastric tumorigenesis, playing an important role in activation of STAT3.

*Corresponding author Wael El-Rifai, M.D., Ph.D., Rosenstiel Med Science Bldg., 1600 NW 10th Ave, Room 4007, Miami, FL 33136-1015, wxe45@miami.edu.

Declaration of Interests: The authors declare no competing interests.

Keywords

Darpp-32; organoids; mouse; human; cancer

Introduction

Although the incidence of gastric cancer has declined in the past few decades, it remains the third leading cause of cancer-associated deaths worldwide[31]. Overexpression of Dopamine and cAMP-regulated phosphoprotein, Mr 32000 (DARPP-32) has been reported as an early step in gastric tumorigenesis, present in intestinal metaplasia, suggesting that DARPP-32 may take part in the transition from atrophic gastritis to intestinal metaplasia and progression to neoplasia [11, 25]. Recent studies have validated that DARPP-32 promotes cancer cell survival, angiogenesis, drug resistance, and invasion[4, 5, 8, 32, 40]. However, the molecular mechanisms by which DARPP-32 promotes gastric tumorigenesis remain unclear.

Chronic inflammation and inflammatory responses play important roles at different stages of carcinogenesis, including tumor initiation, progression, invasion, and metastasis[14]. Multiple cytokines, including interleukins and interferons, control Immune and inflammatory systems [38]. Cytokines initiate intracellular signal transduction pathways and activate transcription factors, such as signal transducers and activators of transcription (STATs)[37]. STATs are a family of proteins comprised of critical mediators of immune response to pathogens and inflammation[27]. Among STAT proteins, activation of STAT3 induces cell proliferation, transformation, apoptosis, angiogenesis, and invasion[3, 36]. Therefore, its activation is a serious step in tumor initiation, progression, and metastasis[20]. While STAT3 activation in normal cells is transient, it is persistently phosphorylated and activated in cancer cells due to activation of upstream tyrosine kinases and/or suppression of its negative regulators[10].

Insulin-like growth factor (IGF) is one of multiple growth factors that can promote tumor progression and increase the metastatic potential of gastric cancer cells[21]. The IGF1 receptor (IGF1R) can inhibit apoptosis of cancer cells through the activation of pro-survival signaling pathways such as SRC, MAP/ERK, and PI3K/AKT [9, 22]. Furthermore, in some cancers, enhanced IGF1R expression can be a pre-requisite for cells to undergo transformation and proliferation[34]. Elevated IGF1R levels can also promote cell survival and metastasis following chemotherapy, leading to reduced survival of gastric cancer patients[16]. Tumor xenograft studies demonstrate that blockade of IGFIR can suppress tumor growth and cancer cell invasion[1]. The fact that amplification and overexpression of IGF1R have been detected in stomach cancers highlights its potential as a therapeutic target[13].

In the present study, we have shown a novel mechanism by which DARPP-32 promotes sustained activation of STAT3 signaling in gastric cancer through interacting with and activating the IGF1R-SRC axis.

Results

DARPP-32 induces STAT3 activity through regulation of IGF1R

Activation of STAT3 transcription network has been reported in early stages of both human and mouse gastric cancer[8]. Overexpression of DARPP-32 has been noted as an early step in gastric tumorigenesis[25]. Therefore, we carried out experiments to determine if DARPP-32 played a role in the activation of STAT3. Transient expression of DARPP-32 in AGS cells, with low endogenous levels, led to an increase in p-STAT3 (Y705) expression (Figure 1A). In contrast, knockdown of endogenous DARPP-32 expression in MKN-45 cells resulted in opposite effects (Figure 1B). We also found that DARPP-32 expression leads to a remarkable increase in p-IGF1R, whereas its knockdown results in complete abrogation of p-IGF1R protein levels (Figure 1A&1B). Of note, knockdown of IGF1R abrogated DARPP-32-induced activation of STAT3 reporter (Figure 1C, $p < 0.01$). Knockdown of endogenous IGF1R or DARPP-32 resulted in a similar reduction of STAT3 reporter activity levels, as compared to controls (Figure 1D, $p < 0.01$).

To confirm activation of STAT3, analysis of the mRNA expression levels of STAT3 target genes demonstrated a significant increase in mRNA levels of *IL6* ($p<0.01$), *c-MYC* ($p<0.01$), *CXCL3* ($p<0.01$) and *IL17* ($p<0.001$) in the DARPP-32 overexpression AGS cells, as compared with control (Figure 2A-2D). In contrast, knockdown of endogenous DARPP-32 expression in MKN-45 cells resulted in opposite effects (Figure 2A-2D), confirming that DARPP-32 was required for expression of these STAT3 target genes. Next, we ruled out GP130 as a downstream effector of DARPP-32 as Western blot data did not reveal notable changes in phospho- or total GP130, following DARPP-32 overexpression (Supplementary figure S1A-S1C). Furthermore, immunoprecipitation and Western blot suggested that DARPP-32 does not interact with GP130 (Supplementary figure S1D), implying that DARPP-32 regulates STAT3 downstream of the IL6R-GP130 complex.

DARPP-32 induces STAT3 activity through IGF1R/SRC signaling pathway

To confirm the role of DARPP-32-IGF1R axis on STAT3 phosphorylation, we performed knockdown of endogenous IGF1R in AGS cells stably expressing DARPP-32. This led to a notable reduction of IGF1R, p-SRC and p-STAT3, as compared to controls cells (Figure 3A), confirming the integrity of this axis in regulating STAT3. Similar results were obtained by using the IGF1R inhibitor OSI-096 (2 μg/ml) and knocking-down endogenous DARPP-32 in MKN45 cells (Figure 3B). STAT3 luciferase reporter assay results, using the same conditions as in 3A & 3B, were in agreement with the aforementioned data (Figure 3C&3D).

Furthermore, we confirmed the role of SRC in regulating DARPP-32-mediated STAT3 activity. Knockdown of endogenous SRC in AGS-pcDNA or AGS-DARPP-32 cells resulted in a decrease in p-SRC and p-STAT3 levels, as compared to controls cells (Figure 4A). Similarly, the use of SRC inhibitor Dasatinib (10 μM) blocked the DARPP-32-induced p-SRC, and p-STAT3, as compared to controls cells (Figure 4B & 4C, $p<0.01$). The use of Dasatinib alone or in combination with knockdown of DARPP-32 resulted in a significant decrease in p-STAT3 (Y705) and its reporter activity (Figure 4D&4E, $p < 0.01$). There were

no significant changes in *SRC* and *IGF1R* mRNA levels following overexpression or knockdown of DARPP-32 (Supplementary figure S2). Immunofluorescence analysis confirmed these findings by showing high levels of p-SRC (Y416) expression in AGS-DARPP-32 cells that were markedly reduced following knockdown of endogenous DARPP-32 (Figure 4F).

DARPP-32 regulates IGFR-SRC pathway

We next utilized dual co-immunoprecipitation to investigate whether DARPP-32 enhances STAT3 activity through protein-protein interaction with IGF1R. We found that DARPP-32 co-exists with IGF1R (Figure 5A), but not with SRC (Supplementary figure S3A-S3B). We used *in situ* proximity ligation assay (PLA) assay to test interaction between endogenous DARPP-32 and IGF1R. We detected a positive ligation, visualized by red immunofluorescence signals, indicative of their close interaction in MKN-45 cells (Figure 5B). These signals were absent in the negative control as well as in PLA control using single DARPP-32 or IGF1R immunofluorescence. These results indicated that DARPP-32 and IGF1R bind to each other and co-exist in the same protein complex, a step that is essential for constitutive phosphorylation of IGF1R (Y1135). Because SRC is a downstream substrate for IGF1R[9], we also investigated if DARPP-32 can also enhance the interaction between IGF1R and SRC to facilitate SRC phosphorylation. The co-immunoprecipitation experiments showed that knockdown DARPP-32 can not decrease IGF1R-SRC interaction (Supplementary Figure S3C), but decreases the interaction between IGF1R and p-SRC (Figure 5C), which is in agreement with the reduced IGF1R phosphorylation, upstream of SRC, following knockdown of DARPP-32 (Figure 3B).

Collectively, these results uncover a novel mechanism that activates STAT3 in gastric cancer cells where DARPP-32–IGF1R–SRC axis is essential for mediating STAT3 activation through phosphorylation of SRC.

DARPP-32 mediates activation of IGF1R - STAT3 axis *in vivo*

To verify the role of DARPP-32 in activation of STAT3 *in vivo*, we performed successful crossings of the DARPP-32 (DP) knockout (KO) mouse model with the TFF1 KO mouse model and obtained double knockout mice (TFF1 KO/DP KO) and determined histological changes in 3 age groups (3, 6, 9–12 months). The TFF1 KO mouse model developed gastric lesions in the range of low-grade dysplasia, high-grade dysplasia, and adenocarcinoma[29].

Using organoid tissue cultures from antral stomach regions, we demonstrated that organoids from the TFF1 KO mice have higher p-IGF1R expression and p-STAT3 nuclear immunostaining than in the DP KO and TFF1 KO/DP KO groups (Figure 6A, supplementary Figure 6). To confirm activation of STAT3, examination of the STAT3 target genes mRNA expression levels demonstrated a significant increase in mRNA levels of *Il6* ($p<0.01$), *c-Myc* ($p<0.01$), *Cxcl3* ($p<0.01$) and *Il17* ($p<0.001$) in the TFF1 KO mice, as compared with wild-type mice. On the other hand, the TFF1 KO/DP KO gastric tissues demonstrated expression levels comparable to wild-type mice (Supplementary figure S4A-S4D), confirming that DARPP-32 was required for expression of these STAT3 target genes. Gross pathology of the stomach revealed nodular mucosa in the glandular antropyloric of the

stomach in TFF1 KO mice at the age of 3–4 months, whereas wild-type, DP KO and TFF1 KO/DP KO mice had no visual lesions (Supplementary figure S5). H&E staining of representative histological features of gastric mucosa showed non-dysplastic gastric glands in wild-type, DP KO and TFF1 KO/DP KO mice, whereas dysplastic glands were observed in TFF1 KO mice (Figure 6B). This suggested that DARPP-32 was required for tumorigenesis at an early age in the TFF1 KO mice. Immunohistochemistry (IHC) staining of p-STAT3 (Y705) and DARPP-32 showed that gastric tissues from the TFF1 KO/DP KO mice had lower levels of p-STAT3 at the age of 2–4 months, as compared to the TFF1 KO mice (Figure 6B). Consistent with these findings, Western blot analysis of the glandular gastric tissue showed that TFF1 KO/DP KO mouse models had lower levels of p-IGF1R, p-SRC and p-STAT3 at the age of 2–4 months, as compared to the TFF1 KO mice (Figure 6C). This confirmed the role of DARPP-32 in regulating IGF1R and suggesting that phosphorylation of STAT3 in the TFF1 KO/DP KO. Furthermore, we found that the TFF1 KO/DP KO mouse model had a significantly lower incidence of low-grade dysplasia (LGD) at the age of 3 months, as compared to the TFF1 KO mouse model (Figure 6D).

The results of immunohistochemistry (IHC) staining on human gastric tissue samples showed weak immunostaining of p–STAT3 (Y705) and DARPP-32 in normal gastric mucosa (Figure 7A). On the contrary, strong immunostaining of p–STAT3 and DARPP-32 were observed in adenocarcinomas (Figure 7A). Using a composite expression score (CES) as described in the Methods section, the IHC data demonstrated a significant increase in expression of p-STAT3 and DARPP-32 ($P<0.01$) in gastric tumors (Figure 7B&7C). Survival analysis by Kaplan-Meier and log rank test, using public data (http://kmplot.com/analysis/index.php?p=service)[30], demonstrated that patients with low expression of DARPP-32 or STAT3 had an overall better survival than those with high expression ($P = 0.05$ and $P = 0.004$, respectively, Figure 7D). Our results from *in vitro*, mouse and human models support the link between p-STAT3 activation and DARPP-32 expression in gastric carcinogenesis. A diagram summarizing our findings is shown in Figure 7E.

Discussion

DARPP-32 overexpression has been recognized in more than 70% of gastric cancers[11, 25] in addition to several other malignancies such as esophageal and colorectal cancers[4, 33]. Dysregulation of various components of JAK2/STAT3 signaling pathways is involved in the development and progression of cancer including gastric, and esophageal carcinoma[2, 26]. For the first time, our study identifies the mechanistic relationship between DARPP-32 and STAT3 in gastric tumorigenesis.

Upon activation by a wide variety of cell surface receptors, STAT3 is phosphorylated[24] and plays an important role in tumorigenesis by promoting cell survival, proliferation, cell cycle progression, and metastasis[6]. Our findings indicate that DARPP-32 mediates phosphorylation of STAT3, an effect that is significantly enhanced following stimulation with IL6. Although GP130 is part of the IL6/IL6R signaling complex that plays an essential role in phosphorylation and activation of JAK/STAT3 signaling axis[18], our findings suggest that DARPP-32 does not interact with the IL6-IL6R-GP130 signaling complex. Therefore, we extended our studies to determine the mechanisms by which DARPP-32 activates

STAT3. We uncovered a previously unknown role of DARPP-32 in phosphorylation and activation of IGF1R and its downstream effector SRC. The IGF1R belongs to the RTK's family and shares 70% homology with the insulin receptor[23]. Overexpression of IGF1R has been observed in many cancers, including esophageal cancer[2], breast cancer[7], and gastric cancer[16, 26]. Our results indicate that DARPP-32 interacted with IGF1R and enhanced IGF1R/p-SRC interaction, providing an explanation for IL6-dependent and independent activation of STAT3 by DARTPP-32. We report that DARPP-32 co-localizes with IGF1R in the same protein complex, a novel finding that significantly adds to the existing data showing that STAT3 can be activated by IGF1/IGF1R signaling[35]. Indeed, pharmacologic inhibition or genetic knockdown of SRC abrogated DARPP-32 mediated activation of STAT3.

Our next step in this study was to investigate the impact of DARPP-32 on gastric tumorigenesis *in vivo.* Earliar, we have reported that DARPP-32 is overexpressed in early stages of human gastric tumorigenesis, as early as intestinal metaplasia[39]. High levels of DARPP-32 are detectable in the gastric mucosa of the TFF1 KO that develops progressive gastric lesions, low grade dysplasia, high grade dysplasia, and cancer[17, 29]. In this study, we found that the TFF1 KO/DP KO mice have absent to low p-STAT3, p-IGF1R, and p-SRC protein levels in gastric mucosa. Of note, we detected a significantly lower incidence of LGD at the age of 3–4 months in these mice, as compared to the TFF1 KO mice. These results suggest that lack of DARPP-32 expression delays the development of gastric tumors in the TFF1 KO mice. This is possibly due to the strong pre-neoplastic phenotype associated with loss of TFF1 and the development of alternate pathways that bypass the DARPP-32-dependent activation of STAT3 over time.

STAT3 and NF-κB activation and interaction play important roles in the control of the communication between inflammatory cells and cancer cells[15]. The cross talks between NF-kB and STAT3 control several oncogenic functions such as cell survival, proliferation, angiogenesis, and invasion[41]. Induction of pro-inflammatory NF-kB signaling is an early step in gastric tumorigenesis due to infection with *H. pylori* or loss of TFF1 protein[29, 41]. A recent study has shown that NF-κB regulates DARPP-32 transcription and expression by bind to the DARPP-32 promoter in gastric cancer cells *in vitro* and *in vivo*[41]. Therefore, it is plausible to conclude that DARPP-32 serves as a bridge between NF-kB and STAT3 where activation of NF-kB in gastric tumorigenesis induces expression of DARPP-32 that subsequently feeds back into this oncogenic pro-inflammatory loop by activating and maintaining the activity of STAT3. Our findings indicate that DARPP-32 plays an essential role in activating and maintaining the activity of STAT3 in gastric cancer cells. This finding is especially important in the context of the existing link between chronic inflammation and cancer[14]. Our observation of the relationship between DARPP-32 and STAT3 provide a promising explanation for the aberrantly high expression of DARPP-32 in gastric cancer cells from tumor-associated inflammation. Collectively, overexpression of DARPP-32 provides a reasonable explanation and highlights a innovative mechanism for IGF1R-SRC dependent activation of the STAT3 pathway in gastric cancer.

In conclusion, our findings indicate that DARPP-32 binds to and activates IGF1R/SRC signaling axis to promote sustained activation of STAT3, a major step in gastric

tumorigenesis. We also found an association between high levels of DARPP-32 and poor clinical outcome. The future development of drugs and therapeutic strategies that target DARPP-32 or its signaling axes may be effective in the treatment of gastric cancer patients.

Materials and Methods

Cell culture and reagents

AGS cells were obtained from American Type Culture Collection (ATCC, Manassas, VA). MKN-45 cells were purchased from the Riken Cell Bank (Tsukuba, Japan). AGS cells were cultured in F12 media (GIBCO, Carlsbad, CA) supplemented with 5% fetal bovine serum (FBS, Invitrogen Life Technologies, Carlsbad, CA) and 1% penicillin/streptomycin (GIBCO). MKN-45 were cultured in Dulbecco's modified Eagle's medium (GIBCO) supplemented with 10% FBS and 1% penicillin/streptomycin. All cell lines were authenticated using short tandem repeat (STR) profiling (Genetica DNA Laboratories, Burlington, NC) to conform to the original *in vitro* morphological characteristics. JAK2 (3230s), p-JAK2 (3776s), p-STAT3 (Y705, 9193s), STAT3 (4904s), p-SRC (Y416, 6943s), SRC (2109), p-IGF1R (Y1135/1136, 3024s), IGF1R (9750s), β-actin (4970) and horseradish peroxidase-conjugated anti-mouse (7074P2) and anti-rabbit (7062P2) secondary antibodies were obtained from Cell Signaling Technology (Danvers, MA). GP130 (sc-655), p-GP130 (sc-22346), and DARPP-32 (sc-398144) antibodies were obtained from Santa Cruz Biotechnology (Santa Cruz, CA). Recombinant Human IL-6 was purchased from PeproTech (Rocky Hill, NJ). Dasatinib and OSI-096 were purchased from Selleck Chemicals (Houston, TX).

DARPP-32 expression and knockdown

PcDNA3.1 expression plasmid was used to clone the FLAG-tagged DARPP-32 cDNA sequence (Invitrogen). Stably expressing pcDNA3.1 or DARPP-32 gastric cancer cells were generated following standard protocols as previously described[5, 11]. Control siRNA (universal negative control1) was obtained from Sigma-Aldrich (St. Louis, MO); Lentivirus particles expressing DARPP-32 shRNA or control shRNA were produced by GeneCopoeia (Rockville, MD) and then utilized to transduce cells. DARPP-32 siRNA (sc-35173), SRC siRNA (sc-29228), and IGF1R siRNA (sc-29358) were purchased from Santa Cruz Biotechnology (Santa Cruz).

Luciferase assay

Cells were transfected with STAT3-LUC luciferase reporter using the DNAfectin Transfection Reagent (Applied Biological Materials, Richmond, BC) in 12-well plates. The luciferase assays were performed using a luciferase assay kit (Promega) according to the manufacturer's protocol. β-galactosidase was used for normalization. Each transfection was performed in triplicate. Measurements using a Luminometer (BMG LABTECH) were conducted following the manufacturer's protocol. Each transfection was performed in triplicate.

Quantitative real-time PCR analysis

Total RNA was isolated from cell lines by using the RNeasy Mini Kit (Qiagen, Valencia, CA). By using an iScript cDNA synthesis kit (Bio-Rad, Hercules, CA), 1 μg RNA was reverse transcribed. Using a Bio-Rad CFX Connect Real-Time System (Bio-Rad), the quantitative real-time PCR (qRT-PCR) was executed. The threshold cycle number was calculated by Bio-Rad CFX manager software version 3.0. All primers were obtained from Integrated DNA Technologies (Supplementary Table 1). All the qRT-PCR reactions were performed in duplicate in three independent experiments. Using the $_{\Delta\Delta}$C(t) method, we calculated fold change[28]. For normalization, we used HPRT1 as a control.

Immunoprecipitation and Western blotting

Cells were lysed with RIPA buffer complemented with protease and phosphatase inhibitors that were purchased from Santa Cruz. Immunoprecipitations were performed at room temperature using equal amounts of total protein for 75 min, by using a primary antibody bounding to 50 μl of Protein A Dynabeads (Invitrogen). Briefly, the beads were washed four times with a wash buffer. This was followed by heating beads in each tube to 95°C for 5 min in 30 μl of sample buffer, followed by magnet separation. 12.5% SDS-PAGE was used to separate proteins and transferred to Immobilon PVDF membrane (Millipore).

Western blotting analysis was performed using laboratory standard methods. For control, we measured protein concentrations and used β-actin as a loading control. All blots were imaged using Bio-Rad ChemiDoc™ XRS+ System (Bio-Rad).

In situ proximity ligation assay (PLA)

To validate the close proximity (<40 nm) between two proteins in gastric cancer cells, PLA was achieved by using Duo-link In Situ-Fluorescence kits according to the manufacturer's instructions (Sigma-Aldrich). The MKN45 cells were grown on 8 chamber slides (Corning, New York, 354108), fixed in 4% paraformaldehyde, and permeabilized using 0.1% Triton-X-100. Cells were then incubated with blocking solution for 1h and incubated overnight with primary antibodies at 4°C (anti-DARPP-32 (sc-398144), Santa Cruz) plus anti-IGF1R (IGF1R (9750s), Cell Signaling,). The cells were subsequently incubated with PLA PLUS and MINUS probes for mouse and rabbit and incubated with ligation-ligase solution for 60 min at 37 °C, and subsequently with amplification-polymerase solution according to the manufacturer's instructions. By mounting solution with DAPI, the slides were mounted. Each red spot represents the close proximity of two interacting proteins. Cell images were obtained using an Inverted laser-scanning LSM880-Airyscan (Zeiss, Thornwood, NY) confocal microscope.

Immunofluorescence

Immunofluorescence was performed following cell fixation and permeabilization, using antibodies against DARPP-32 (1:400) (Santa Cruz, sc-398144), p-STAT3 (Cell Signaling, Y705, 9193s) or p-SRC (1:400) (Cell Signaling, Y416, 6943s). The cells were washed with cold PBS three times for 5 min each, and incubated with both Alexa Fluor goat anti-mouse IgG and Alexa Fluor goat anti-rabbit IgG (1:800) (Invitrogen) at room temperature for 90

min. Cell images were acquired using an Inverted laser-scanning LSM880-Airyscan (Zeiss, Thornwood, NY) confocal microscope.

Tissue microarray and immunohistochemistry

A total of 216 paraffin-embedded human gastric tissue samples (108 normal and 108 adenocarcinomas) were presented for immunohistochemical analysis. In accordance with approved protocols, all tissue samples were obtained coded and de-identified. Tissues were stained with hematoxylin and eosin. Representative regions were marked by our pathologist and selected for inclusion in a tissue array. Sections (5 μm) were transferred to poly lysine-coated slides (SuperFrostPlus; Menzel-Glaser, Braunschweig, Germany) and incubated at 37°C for 2 hrs. For deparaffinization, paraffin-embedded tissues were pretreated at 65°C for 2 hrs and standard procedures were followed. For antigen retrieval, we used a solution of 1 mmol/L EDTA, 10 mmol/L Tris, pH 8.0. DARPP-32 (F3) antibody from Santa Cruz Biotechnology and p-STAT3 (Y705, ab76315, Cambridge, MA) antibody were used in IHC staining. Slides were incubated overnight at 4°C for primary antibody followed by washed with PBS plus 0.1% Tween 20 three times, and additional 1 h incubation at room temperature with the secondary antibody. Horseradish peroxidase activity was identified using a Histostain Plus kit (Invitrogen), following supplier's instructions. Tumor tissue sections were counterstained with hematoxylin and mounted. The immunoreactivity of tested samples was assessed by a trained pathologist and scored for intensity (scaled 0–3) and frequency (scaled 0–4). Composite expression score (CES) was calculated utilizing the formula CES = Intensity × Frequency. The range of CES was from 0 to 12 [25, 29].

Gastric organoids

The mouse stomach was cut into 2–3 mm pieces on ice with cold PBS and then incubated in 1 ml of 5 mM EDTA for 30 min at 37°C with shaking and centrifuged at 1,500 rpm for 5 min at 4°C. The cell suspension was filtered through a 70 μM filter. This was followed by centrifugation of the crypts fraction at 1,500 rpm for 10 min at 4°C. The pellet was resuspended in 5 ml ice-cold PBS. The crypts were centrifuged and the pellet was suspended in 50 μl Matrigel (BD Biosciences) and plated in pre-warmed 24-well plates. The matrigel was allowed to solidify for 20 min in the tissue culture incubator, 500 μl mouse basal medium (STEMCELL, 06000, Cambridge, MA) was overlaid, and media was replaced every 4 days. Organoids were collected after 14 days, fixed in 4% PFA for 20 min, washed in 1× PBS and re-suspended in 30 μl of Histo-gel (Richard-Allan) and mixed with the cell pallet. Carefully, we removed the histo-gel dome from the tube, placed the dome into a cassette and placed into 70% ethanol then processed for paraffin embedding. Paraffin-embedded organoids were pretreated at 65°C for 2h, following by deparaffinization procedures. Antigen retrieval was performed using a solution of 10 mmol/L Tris, 1 mmol/L EDTA, pH 8.0. Slides were then incubated for primary antibody overnight at 4°C followed by washes with PBST (PBS plus 0.1% Tween 20) three times, and then incubated with both Alexa Fluor goat anti-rabbit IgG and Alexa Fluor goat anti-mouse IgG (1:800) (Invitrogen) at room temperature for 2 h. Images were acquired using an inverted laser-scanning LSM880-Airyscan (Zeiss, Thornwood, NY) confocal microscope.

Animals

Darpp-32 knockout mice (DP KO) were a kind gift from Dr. Paul Greengard's laboratory at The Rockefeller University[12]. The TFF1 KO mice were used as models of gastric tumorigenesis[19, 29]. The TFF1 KO/DP KO double-knockout mice. All animals were approved by the Institutional Animal Care and Use Committee at Vanderbilt University and University of Miami (IACUC protocols M1500061 and 17–134). According to the protocol, the animals were dissected through midline incisions of the abdomen following euthanasia. The stomachs were examined visually for abnormalities and size. Individual gastric tumors were photographed. Formalin-fixed paraffin-embedded and frozen stomach tissue samples were gathered from TFF1 KO/DP KO (n=37), TFF1 KO (n=54), DP KO (n=11), and wild-type mice (n=21). All mice were of C57/B6/S129 mixed background. Classification and grading of the gastric tissues were performed by our pathologists on the study. The remaining half of the stomach was snap-frozen and stored at −80°C for further use.

Statistics

Data was expressed as mean ± SD of three independent experiments. Statistical analysis was conducted with the GraphPad Prism 5. Statistical significance of the *in vitro* and *in vivo* studies was analyzed by the Student's *t* test, one-way ANOVA, and Pearson's method. The grouped data was analyzed with the one-way ANOVA and a 2-tailed Student's t-test was used to compare the statistical difference between the two groups. Significance is described in the figure legends as $P< 0.05$; $P< 0.01$.

Supplementary Material

Refer to Web version on PubMed Central for supplementary material.

Acknowledgments:

Grant Support: This study was supported by the U.S. National Institutes of Health (R01CA93999), Research Career Scientist award (1IK6BX003787), and a merit award (I01BX001179) from the U.S. Department of Veterans affairs (W. El-Rifai). The contents of this work are solely the responsibility of the authors and do not necessarily represent the official views of the Department of Veterans Affairs, National Institutes of Health, or the University of Miami.

REFERENCES

1. Adachi Y, Li R, Yamamoto H, Min Y, Piao W, Wang Y et al. Insulin-like growth factor-I receptor blockade reduces the invasiveness of gastrointestinal cancers via blocking production of matrilysin. Carcinogenesis 2009; 30: 1305–1313. [PubMed: 19493905]
2. Adachi Y, Ohashi H, Imsumran A, Yamamoto H, Matsunaga Y, Taniguchi H et al. The effect of IGF-I receptor blockade for human esophageal squamous cell carcinoma and adenocarcinoma. Tumour Biol 2014; 35: 973–985. [PubMed: 24026884]
3. Ahn JH, Choi YS, Choi JH. Leptin promotes human endometriotic cell migration and invasion by up-regulating MMP-2 through the JAK2/STAT3 signaling pathway. Mol Hum Reprod 2015; 21: 792–802. [PubMed: 26153131]
4. Beckler A, Moskaluk CA, Zaika A, Hampton GM, Powell SM, Frierson HF Jr. et al. Overexpression of the 32-kilodalton dopamine and cyclic adenosine 3',5'-monophosphate-regulated phosphoprotein in common adenocarcinomas. Cancer 2003; 98: 1547–1551. [PubMed: 14508844]

5. Belkhiri A, Zaika A, Pidkovka N, Knuutila S, Moskaluk C, El-Rifai W. Darpp-32: a novel antiapoptotic gene in upper gastrointestinal carcinomas. Cancer Res 2005; 65: 6583–6592. [PubMed: 16061638]
6. Cafferkey C, Chau I. Novel STAT 3 inhibitors for treating gastric cancer. Expert Opin Investig Drugs 2016; 25: 1023–1031.
7. Carboni JM, Lee AV, Hadsell DL, Rowley BR, Lee FY, Bol DK et al. Tumor development by transgenic expression of a constitutively active insulin-like growth factor I receptor. Cancer Res 2005; 65: 3781–3787. [PubMed: 15867374]
8. Chen Z, Zhu S, Hong J, Soutto M, Peng D, Belkhiri A et al. Gastric tumour-derived ANGPT2 regulation by DARPP-32 promotes angiogenesis. Gut 2016; 65: 925–934. [PubMed: 25779598]
9. Chen Z, Soutto M, Rahman B, Fazili MW, Peng D, Blanca Piazuelo M et al. Integrated expression analysis identifies transcription networks in mouse and human gastric neoplasia. Genes Chromosomes Cancer 2017; 56: 535–547. [PubMed: 28281307]
10. Darnell JE Jr. STATs and gene regulation. Science 1997; 277: 1630–1635. [PubMed: 9287210]
11. El-Rifai W, Smith MF Jr., Li G, Beckler A, Carl VS, Montgomery E et al. Gastric cancers overexpress DARPP-32 and a novel isoform, t-DARPP. Cancer Res 2002; 62: 4061–4064. [PubMed: 12124342]
12. Fienberg AA, Hiroi N, Mermelstein PG, Song W, Snyder GL, Nishi A et al. DARPP-32: regulator of the efficacy of dopaminergic neurotransmission. Science 1998; 281: 838–842. [PubMed: 9694658]
13. Ge J, Chen Z, Huang J, Yuan W, Den Z. Silencing insulin-like growth factor-1 receptor expression inhibits gastric cancer cell proliferation and invasion. Mol Med Rep 2015; 11: 633–638. [PubMed: 25339573]
14. Grivennikov SI, Greten FR, Karin M. Immunity, inflammation, and cancer. Cell 2010; 140: 883–899. [PubMed: 20303878]
15. Grivennikov SI, Karin M. Dangerous liaisons: STAT3 and NF-kappaB collaboration and crosstalk in cancer. Cytokine Growth Factor Rev 2010; 21: 11–19. [PubMed: 20018552]
16. Gryko M, Kisluk J, Cepowicz D, Zinczuk J, Kamocki Z, Guzinska-Ustymowicz K et al. Expression of insulin-like growth factor receptor type 1 correlate with lymphatic metastases in human gastric cancer. Pol J Pathol 2014; 65: 135–140. [PubMed: 25119174]
17. He G, Karin M. NF-kappaB and STAT3 - key players in liver inflammation and cancer. Cell Res 2011; 21: 159–168. [PubMed: 21187858]
18. Jones SA, Scheller J, Rose-John S. Therapeutic strategies for the clinical blockade of IL-6/gp130 signaling. J Clin Invest 2011; 121: 3375–3383. [PubMed: 21881215]
19. Lefebvre O, Chenard MP, Masson R, Linares J, Dierich A, LeMeur M et al. Gastric mucosa abnormalities and tumorigenesis in mice lacking the pS2 trefoil protein. Science 1996; 274: 259–262. [PubMed: 8824193]
20. Li CJ, Li YC, Zhang DR, Pan JH. Signal transducers and activators of transcription 3 function in lung cancer. J Cancer Res Ther 2013; 9 Suppl 2: S67–73. [PubMed: 24135245]
21. Li S, Lei X, Zhang J, Yang H, Liu J, Xu C. Insulin-like growth factor 1 promotes growth of gastric cancer by inhibiting foxo1 nuclear retention. Tumour Biol 2015; 36: 4519–4523. [PubMed: 25596089]
22. Ma Y, Tang N, Thompson RC, Mobley BC, Clark SW, Sarkaria JN et al. InsR/IGF1R Pathway Mediates Resistance to EGFR Inhibitors in Glioblastoma. Clin Cancer Res 2016; 22: 1767–1776. [PubMed: 26561558]
23. Menting JG, Lawrence CF, Kong GK, Margetts MB, Ward CW, Lawrence MC. Structural Congruency of Ligand Binding to the Insulin and Insulin/Type 1 Insulin-like Growth Factor Hybrid Receptors. Structure 2015; 23: 1271–1282. [PubMed: 26027733]
24. Mitchell TJ, John S. Signal transducer and activator of transcription (STAT) signalling and T-cell lymphomas. Immunology 2005; 114: 301–312. [PubMed: 15720432]
25. Mukherjee K, Peng D, Brifkani Z, Belkhiri A, Pera M, Koyama T et al. Dopamine and cAMP regulated phosphoprotein MW 32 kDa is overexpressed in early stages of gastric tumorigenesis. Surgery 2010; 148: 354–363. [PubMed: 20580047]

26. Numata K, Oshima T, Sakamaki K, Yoshihara K, Aoyama T, Hayashi T et al. Clinical significance of IGF1R gene expression in patients with Stage II/III gastric cancer who receive curative surgery and adjuvant chemotherapy with S-1. J Cancer Res Clin Oncol 2016; 142: 415–422. [PubMed: 26337161]
27. O'Shea JJ, Plenge R. JAK and STAT signaling molecules in immunoregulation and immune-mediated disease. Immunity 2012; 36: 542–550. [PubMed: 22520847]
28. Pfaffl MW. A new mathematical model for relative quantification in real-time RT-PCR. Nucleic Acids Res 2001; 29: e45. [PubMed: 11328886]
29. Soutto M, Belkhiri A, Piazuelo MB, Schneider BG, Peng D, Jiang A et al. Loss of TFF1 is associated with activation of NF-kappaB-mediated inflammation and gastric neoplasia in mice and humans. J Clin Invest 2011; 121: 1753–1767. [PubMed: 21490402]
30. Szasz AM, Lanczky A, Nagy A, Forster S, Hark K, Green JE et al. Cross-validation of survival associated biomarkers in gastric cancer using transcriptomic data of 1,065 patients. Oncotarget 2016; 7: 49322–49333. [PubMed: 27384994]
31. Torre LA, Bray F, Siegel RL, Ferlay J, Lortet-Tieulent J, Jemal A. Global cancer statistics, 2012. CA Cancer J Clin 2015; 65: 87–108. [PubMed: 25651787]
32. Vangamudi B, Peng DF, Cai Q, El-Rifai W, Zheng W, Belkhiri A. t-DARPP regulates phosphatidylinositol-3-kinase-dependent cell growth in breast cancer. Mol Cancer 2010; 9: 240. [PubMed: 20836878]
33. Wang MS, Pan Y, Liu N, Guo C, Hong L, Fan D. Overexpression of DARPP-32 in colorectal adenocarcinoma. Int J Clin Pract 2005; 59: 58–61. [PubMed: 15707466]
34. Werner H Tumor suppressors govern insulin-like growth factor signaling pathways: implications in metabolism and cancer. Oncogene 2012; 31: 2703–2714. [PubMed: 21963847]
35. Yadav A, Kalita A, Dhillon S, Banerjee K. JAK/STAT3 pathway is involved in survival of neurons in response to insulin-like growth factor and negatively regulated by suppressor of cytokine signaling-3. J Biol Chem 2005; 280: 31830–31840. [PubMed: 15998644]
36. Yang C, He L, He P, Liu Y, Wang W, He Y et al. Increased drug resistance in breast cancer by tumor-associated macrophages through IL-10/STAT3/bcl-2 signaling pathway. Med Oncol 2015; 32: 352. [PubMed: 25572805]
37. Yoshimura A, Mori H, Ohishi M, Aki D, Hanada T. Negative regulation of cytokine signaling influences inflammation. Curr Opin Immunol 2003; 15: 704–708. [PubMed: 14630206]
38. Yoshimura A, Nishinakamura H, Matsumura Y, Hanada T. Negative regulation of cytokine signaling and immune responses by SOCS proteins. Arthritis Res Ther 2005; 7: 100–110. [PubMed: 15899058]
39. Zhao G, Zhu G, Huang Y, Zheng W, Hua J, Yang S et al. IL-6 mediates the signal pathway of JAK-STAT3-VEGF-C promoting growth, invasion and lymphangiogenesis in gastric cancer. Oncol Rep 2016; 35: 1787–1795. [PubMed: 26750536]
40. Zhu S, Belkhiri A, El-Rifai W. DARPP-32 Increases Interactions Between Epidermal Growth Factor Receptor and ERBB3 to Promote Tumor Resistance to Gefitinib. Gastroenterology 2011; 141: 1738–1748 e1732. [PubMed: 21741919]
41. Zhu S, Soutto M, Chen Z, Peng D, Romero-Gallo J, Krishna US et al. Helicobacter pylori-induced cell death is counteracted by NF-kappaB-mediated transcription of DARPP-32. Gut 2017; 66: 761–762.

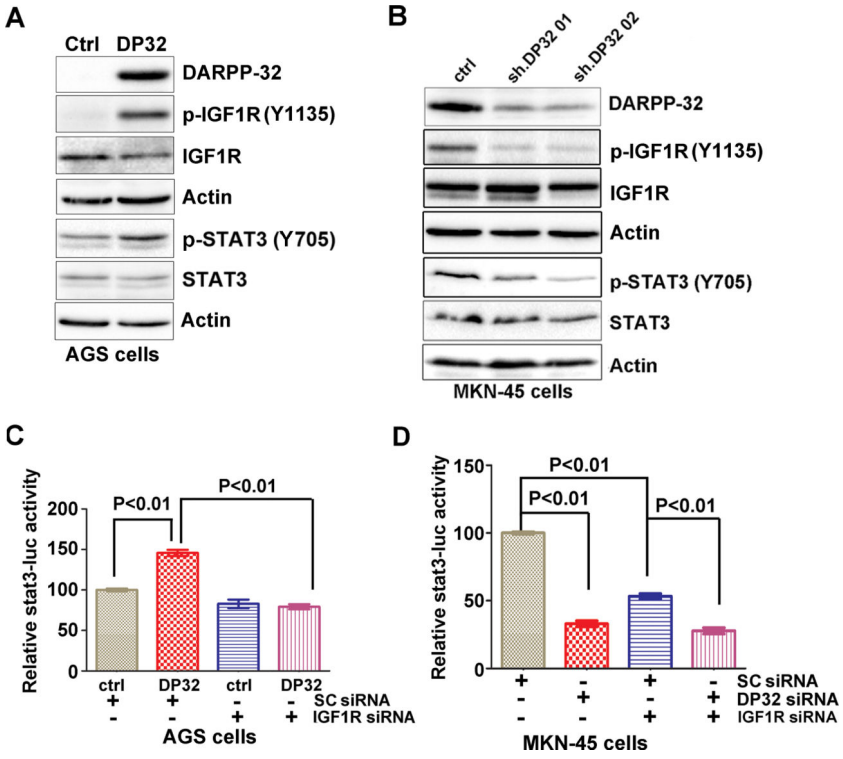

Figure 1. DARPP-32 enhances activation of p-IGF1R.

A-B) p-IGF1R, p-STAT3, and DARPP-32 protein levels were determined by Western blot analysis in AGS cells with stable expression of DARPP-32 (DP32) or MKN45 cells with siRNA knockdown of DARPP-32. C-D) Luciferase reporter assay for STAT3-luc following siRNA knockdown of IGF1R in cells with stable expression of DARPP-32 (DP32) or DARPP-32 siRNA knockdown. Statistical significance in all panels was calculated by the 1-way ANOVA, followed by the Newman-Keuls test.

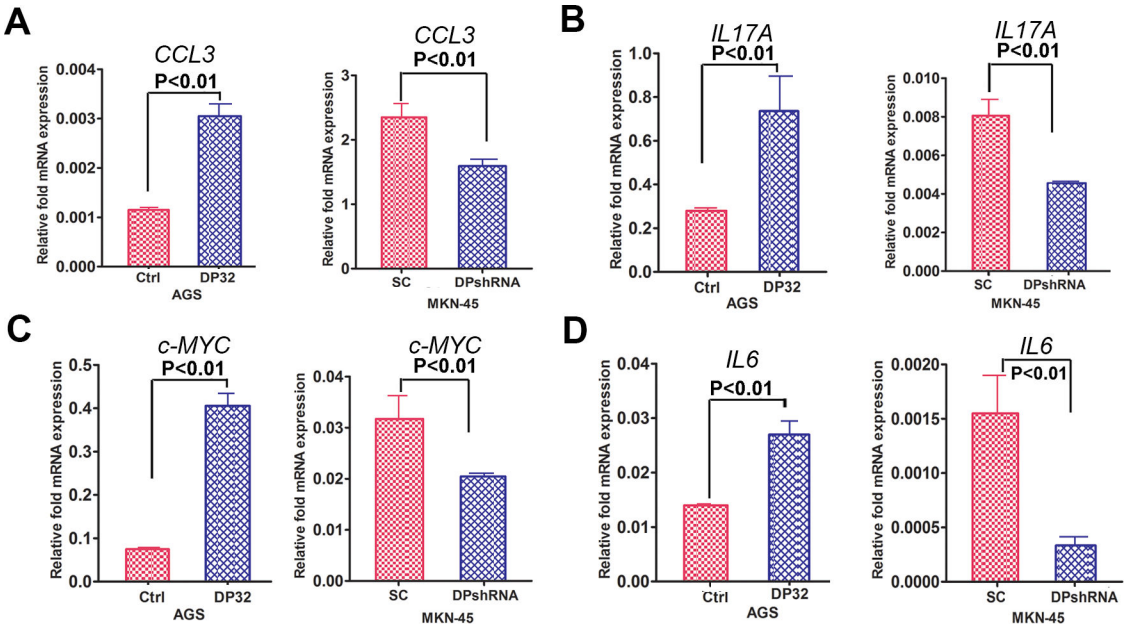

Figure 2. STAT3 targeted genes mRNA expression regulated by DARPP-32.

A-D) The qRT-PCR analysis of IL6, c-MYC, CXCL3 and IL17 expression was performed in AGS cells, following transient expression of DARPP-32 (DP32), using pcDNA-DARPP-32 (AGS) or DARPP-32 shRNA knockdown in MKN45 cells. Statistical significance in all panels was calculated by 1-way ANOVA, followed by the student's t test.

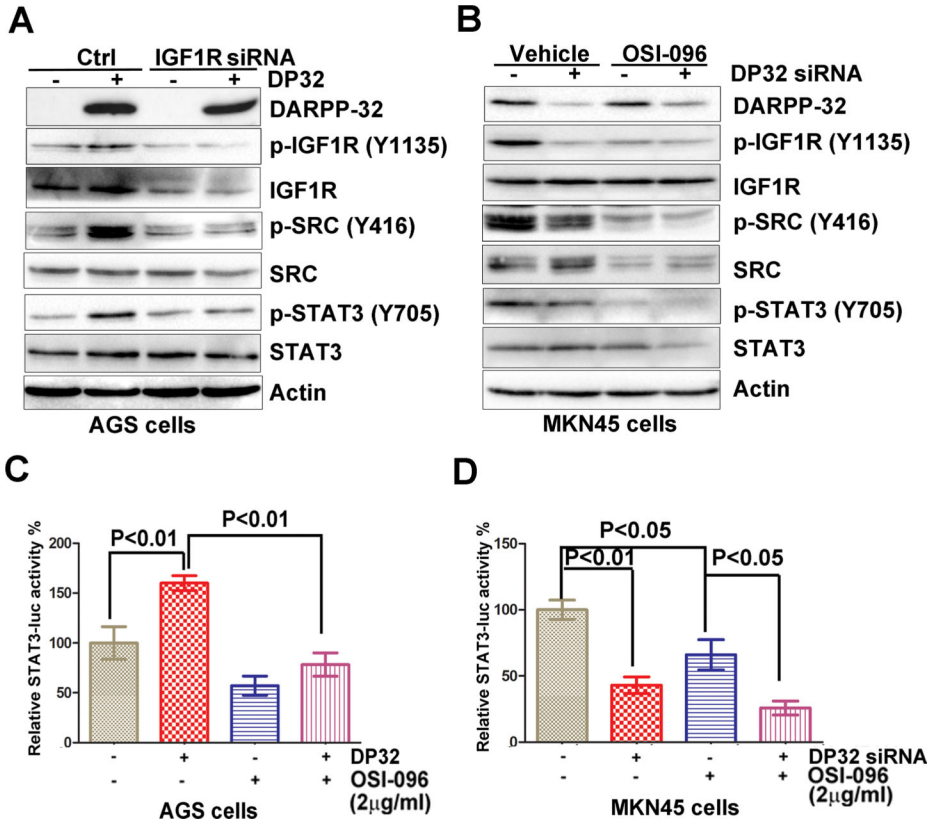

Figure 3. DARPP-32 regulates IGF1R-mediated STAT3 signaling pathway in gastric cancer cells: A) Western blots analysis of IGF1R, p-IGF1R, SRC, and p-SRC in AGS cells stably expressing DARPP-32 (DP32), following IGF1R siRNA knockdown. B) p-IGF1R, SRC, and p-SRC protein levels were determined by Western blot analysis in MKN45 cells, following DARPP-32 siRNA knockdown and treatment with OSI-096 (2 μg/ml) or vehicle. C-D) Luciferase reporter assay for STAT3-luc following treatment with OSI-096 (2 μg/ml) in AGS cells stably expressing DARPP-32 (DP32), using pcDNA-DARPP-32 or DARPP-32 siRNA knockdown in MKN45 cells. Statistical significance in all panels was calculated by 1-way ANOVA, followed by the student's t test.

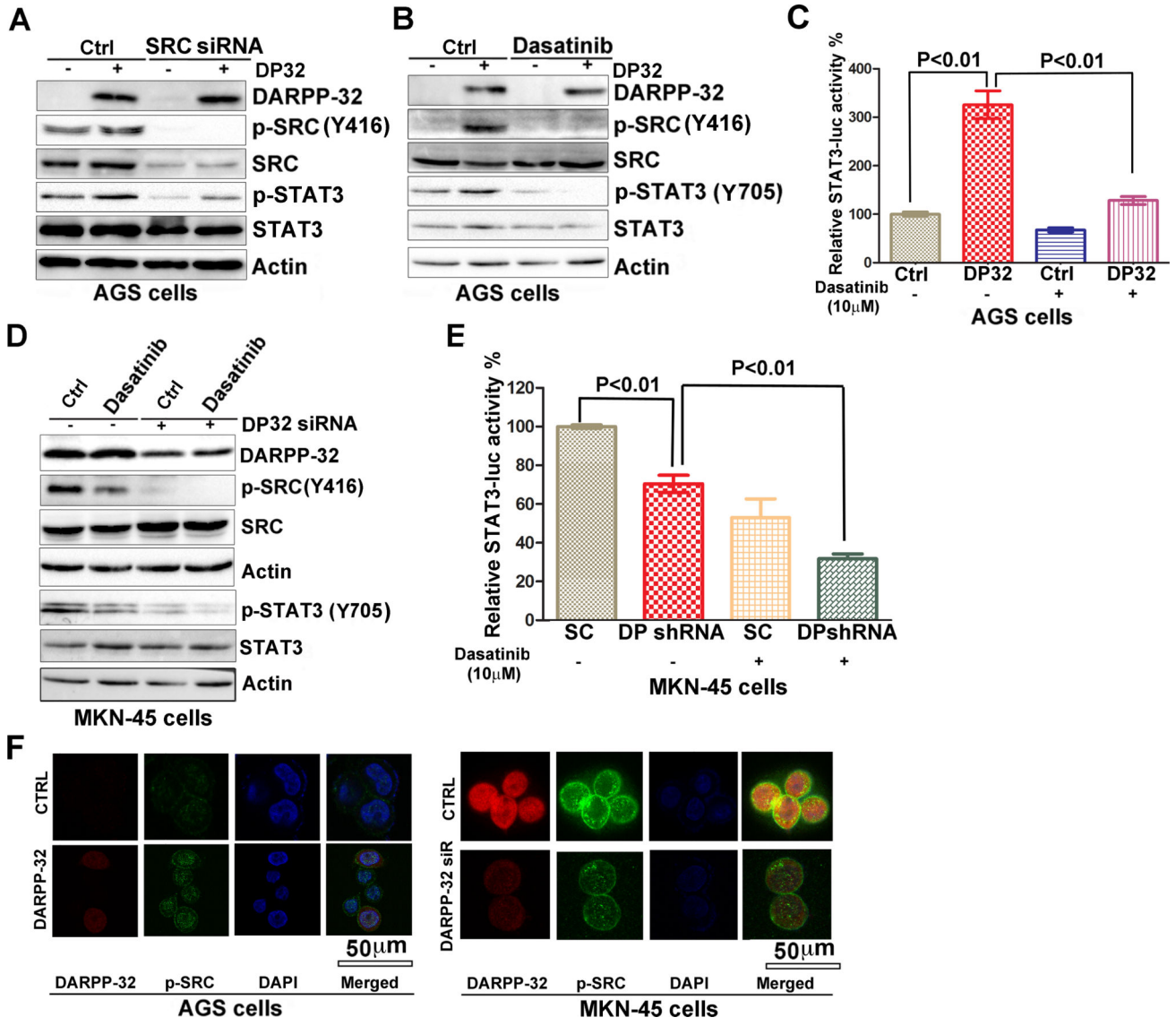

Figure 4. DARPP-32 induces STAT3 activity through SRC signaling pathway.

A) Western blots analysis of p-SRC, p-STAT3, and DARPP-32 in AGS cells stably expressing DARPP-32 (DP32), using pcDNA-DARPP-32, following knockdown of SRC by SRC siRNA. B) p-SRC, p-STAT3, and DARPP-32 protein levels were determined by Western blot analysis in AGS cells stably expressing DARPP-32 (DP32), following treatment with Dasatinib (10 μM) or vehicle. C) Luciferase reporter assays for STAT3-luc were performed following treatment with Dasatinib (10 μM) in AGS cells stably expressing DARPP-32 (DP32). Statistical significance in all panels was calculated by the 1-way ANOVA, followed by the Newman-Keuls test. D) p-SRC, p-STAT3, and DARPP-32 protein levels were determined by Western blot analysis in DARPP-32 siRNA knockdown MKN45 cells following treatment with Dasatinib (10 μM) or vehicle. E) Luciferase reporter assay for STAT3-luc were performed following Dasatinib (10 μM) treatment in DARPP-32 siRNA knockdown MKN45 cells. Statistical significance in all panels was calculated by the 1-way ANOVA, followed by the Newman-Keuls test. F) Immunofluorescence analysis using AGS

cells, following overexpression of DARPP-32 (red), demonstrates an increase in expression of p-SRC (green) in DARPP-32-expressing AGS cells (left panel). Immunofluorescence analysis in MKN45 cells, following DARPP-32 siRNA knockdown, demonstrates a decrease of p-SRC in DARPP-32 siRNA/MKN45 cells; DARPP-32 (red), p-STAT3 (green) (right panel).

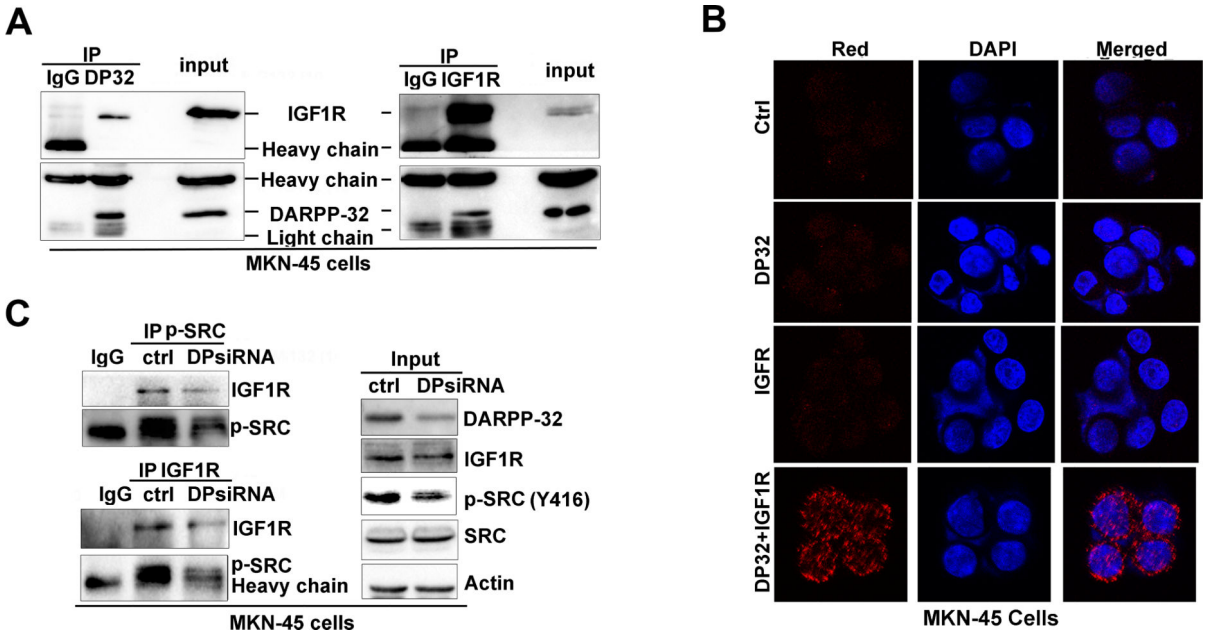

Figure 5. DARPP-32 interacts with IGF1R.

A) Two-way co-immunoprecipitation and Western blot analysis demonstrates the interaction of DARPP-32 and IGF1R. B) in situ proximity ligation assay (PLA) showing co-localization of DARPP-32 with IGF1R (red dots, left panel, bottom row), no ligation signals were seen in controls. C) Using immunoprecipitation of p-SRC and IGF1R, the IGF1R-p-SRC interaction was examined following DARPP-32 siRNA knockdown in MKN45 cells.

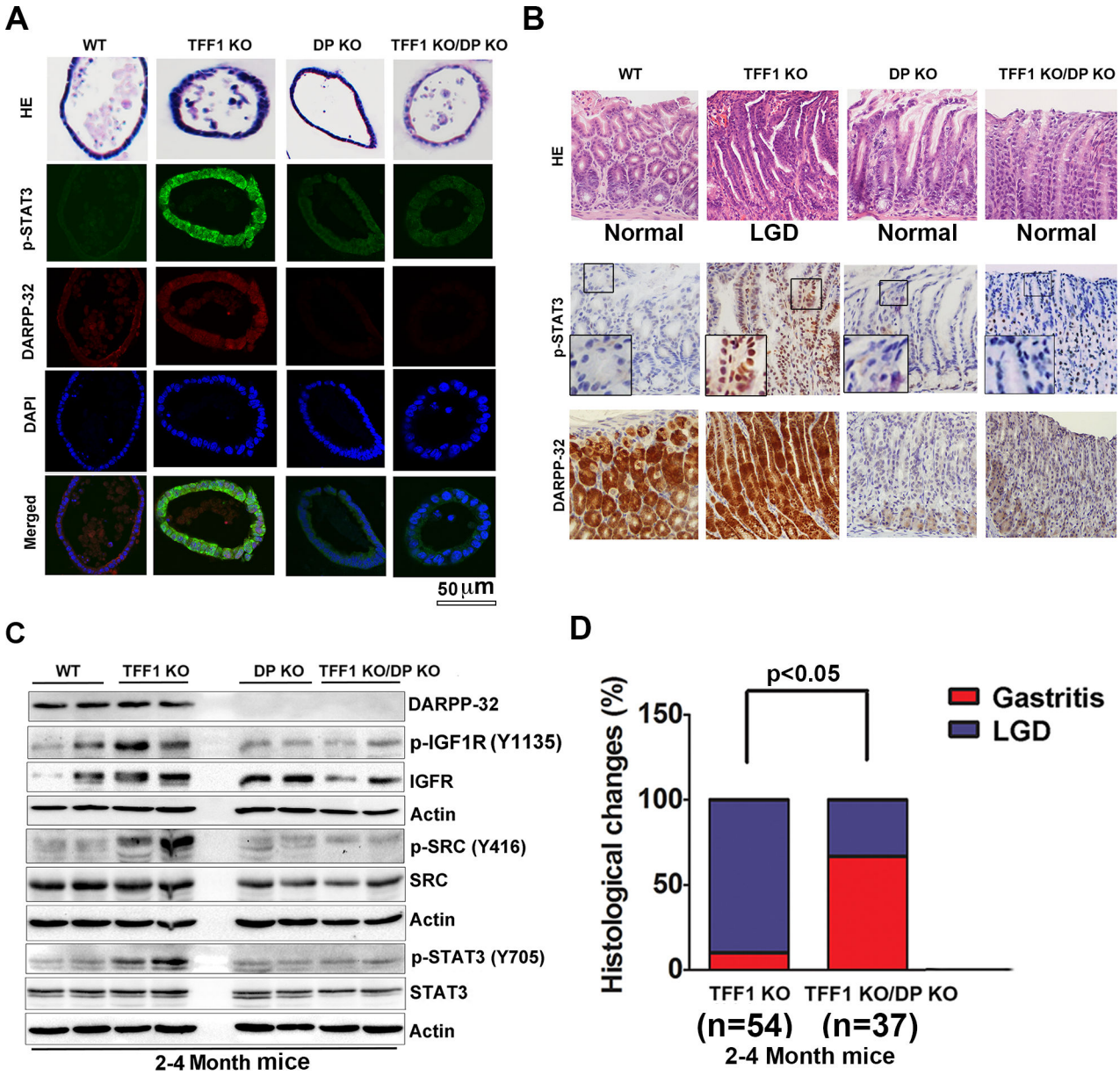

Figure 6. DARPP-32 regulates IGFR-SRC pathway.

A) Immunofluorescence analysis of p-STAT3 (green) and DARPP-32 (red) in gastric organoids established from wild-type, TFF1 KO, DP KO and TFF1 KO/DP KO mice. B) H&E staining of representative histological features of gastric mucosa from 2–4 month old mice; wild-type (n=9), TFF1 KO (n=14), DP KO (n=10), and TFF1 KO/DP KO (n=9). Lack of dysplastic gastric glands in wild-type, DP KO, and TFF1 KO/DP KO mice; dysplastic glands were observed in TFF1 KO mice (upper panel). Representative immune-histochemical staining of DARPP-32 and p-STAT3 in gastric tissues from wild-type, TFF1 KO, DP KO, and TFF1 KO/DP KO 2–4 month old mice (lower panel). C) Western blot analysis of IGFR-SRC pathway in 2–4 month old mice. D) Histological changes were examined in TFF1 KO and TFF1 KO/DP KO old mice. Wild-type mice (n=21), TFF1 KO (n=54), DP KO (n=11), and TFF1 KO/DP KO (n=37) mice were evaluated for chronic

inflammation and dysplasia. Statistical significance in all panels was calculated by the 1-way ANOVA, followed by the Newman-Keuls test.

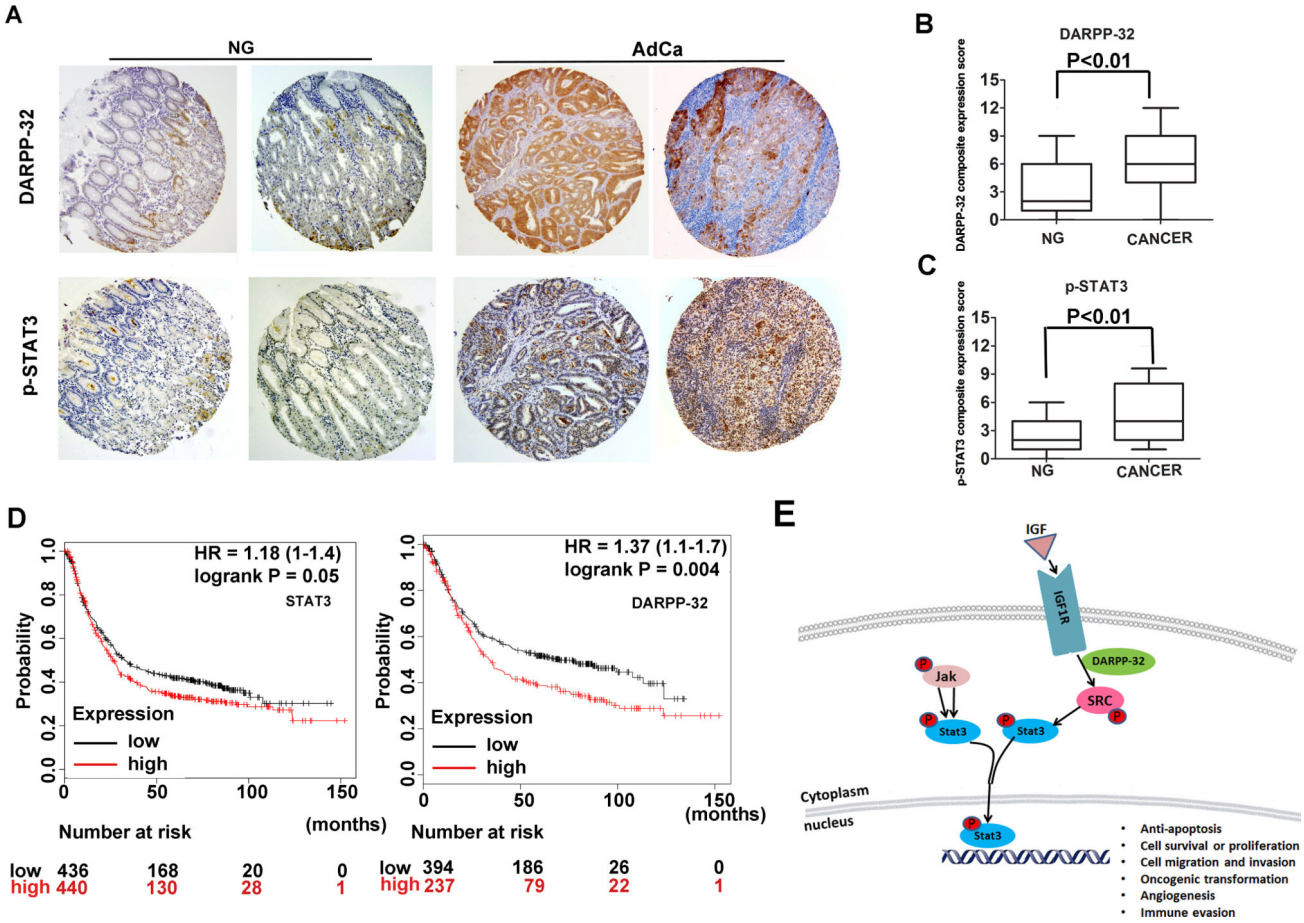

Figure 7. Immunohistochemistry for DARPP-32 and p-STAT3 in human gastric tissues

A) Representative images of immune-histochemical staining of DARPP-32 and p-STAT3 in tissue sections from human gastric mucosa with normal histology (NG, n=108) and adenocarcinoma (AdCa, n=108); original magnification ×20. B-C) The graphs summarize the immunohistochemical staining results on gastric tissue microarrays. D) Survival analysis of DARPP-32 and STAT3 mRNA expression in gastric cancer patients by the Kaplan-Meier survival curve, n=882, following analysis of public data online (http://kmplot.com/analysis/index.php?p=service) [25]. E) A diagram depicting the role of DARPP-32 in activation of STAT3 in gastric cancer cells. In summary, DARPP-32 interacts with IGF1R and promotes IGF1R and SRC phosphorylation, allowing sustained IL6-mediated phosphorylation and activation of STAT3. The translocation of p-STAT3 into the nucleus initiates transcriptional regulation of downstream target genes that regulate cell proliferation, transformation.